ACS APPLIED POLYMER MATERIALS

pubs.acs.org/acsapm Article

Highly Effective Index-Matching Antireflective Structures for Polymer Optics

Sivan Tzadka, Imon Kalyan, Esti Toledo, Yonatan Sivan, and Mark Schvartzman*

Cite This: ACS Appl. Polym. Mater. 2023, 5, 5103−5109 Read Online

ACCESS | Metrics & More | Article Recommendations | Supporting Information

ABSTRACT: Optical polymers are attractive for lightweight and cost-effective refractive optical components, yet they reflect part of the incident light. Traditional vacuum-deposited antireflective films purely adhere to polymers and suffer from mechanical stresses due to the difference in the thermal expansion coefficients. Alternatively, reflection can be reduced by moth-eye structures; yet, their efficiency strongly depends on their index-matching with the optical substrate, which has not been demonstrated so far. Here, we introduce a new approach to engineering highly effective antireflective structures on the surface of the optical polymer, with an unprecedented ability to reduce the surface reflection from 5 to 0.1%. The structures were produced by high-throughput nanoimprint lithography, and their superior optical performance was achieved due to the precise matching of their index to that of the underlying substrate. We further applied these structures on different polymers and showed that their antireflective effect correlates with index-matching. We demonstrated that these structures could be applied on flat surfaces and curved lenses and produce high surface hydrophobicity. Overall, our work paves the way to an efficient and scalable antireflective solution for polymer optics.

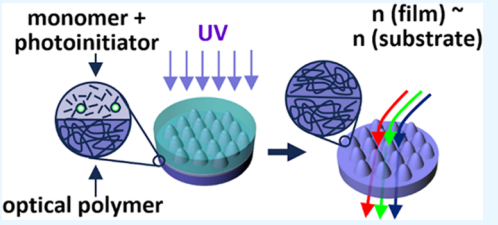

KEYWORDS: *index-matching, polymer optics, UV-nanoimprint, antireflective structures, lenses*

1. INTRODUCTION

Polymers are attractive substitutes for glass as optical materials in the visible spectrum due to the low cost of their raw materials and processing and high optical transparency.[1−3] However, like any optical material, optical polymers reflect part of the incident light, which causes blurriness and white spots and reduces transmission. Currently, a broadly explored solution for reflection from optical surfaces is moth-eye structures that are effective within a broad range of wavelengths and incident angles.[4] An attractive approach to fabricate optical structures in polymers is nanoimprint lithography. Thermal nanoimprint can easily produce optical structures within a polymer film on a solid substrate.[5−9] However, all of the attempts to thermally imprint nanostructures directly on polymer substrates[10−14] ignored the fact that thermal imprint would deform the polymer bulk due to the combination of the applied high pressure and temperature, making such a process incompatible with polymer substrates such as optical windows and lenses, whose shape must be precisely maintained. Therefore, state-of-the-art thermal imprint is not suitable for the fabrication of antireflective structures on polymer-based optical components. Ultraviolet (UV) imprint, on the other hand, is performed at room temperature and thus does not deform the imprinted optical components.[15] Still, all of the attempts to produce UV-imprinted antireflective structures on polymers produced very poor antireflective performance, in which the reflection was still about a few percent.[16−18] Such a reflection is too high for most practical optical applications, and it is much above the theoretical potential of moth-eye structures to reduce reflection.

While state-of-the-art works on polymer antireflective structures are examined, it becomes clear that the reason for their poor antireflective performance stems from the optical properties of the imprinted polymer. Indeed, the fundamental principle of the broadband antireflective structure is that the structures and the underlying substrates have very similar refractive indexes.[4,19−21] This ensures, according to the effective medium theory,[22,23] a smooth gradient of the effective refractive index from air to that of the substrate. The smooth gradient, in turn, produces a highly broadband and omnidirectional antireflective effect, which is analogous to that produced by an infinite number of antireflective films with gradually changing indexes (Figure 1a). Yet, so far, all of the antireflective structures on imprinted polymers were made of materials with random indexes, such as commercially available UV imprint resist.[16,24,25] The refractive indexes of these resists did not match those of the substrates and produced undesirable optical interfaces between the bulk and imprinted

Received: March 23, 2023
Accepted: June 9, 2023
Published: June 22, 2023

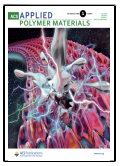

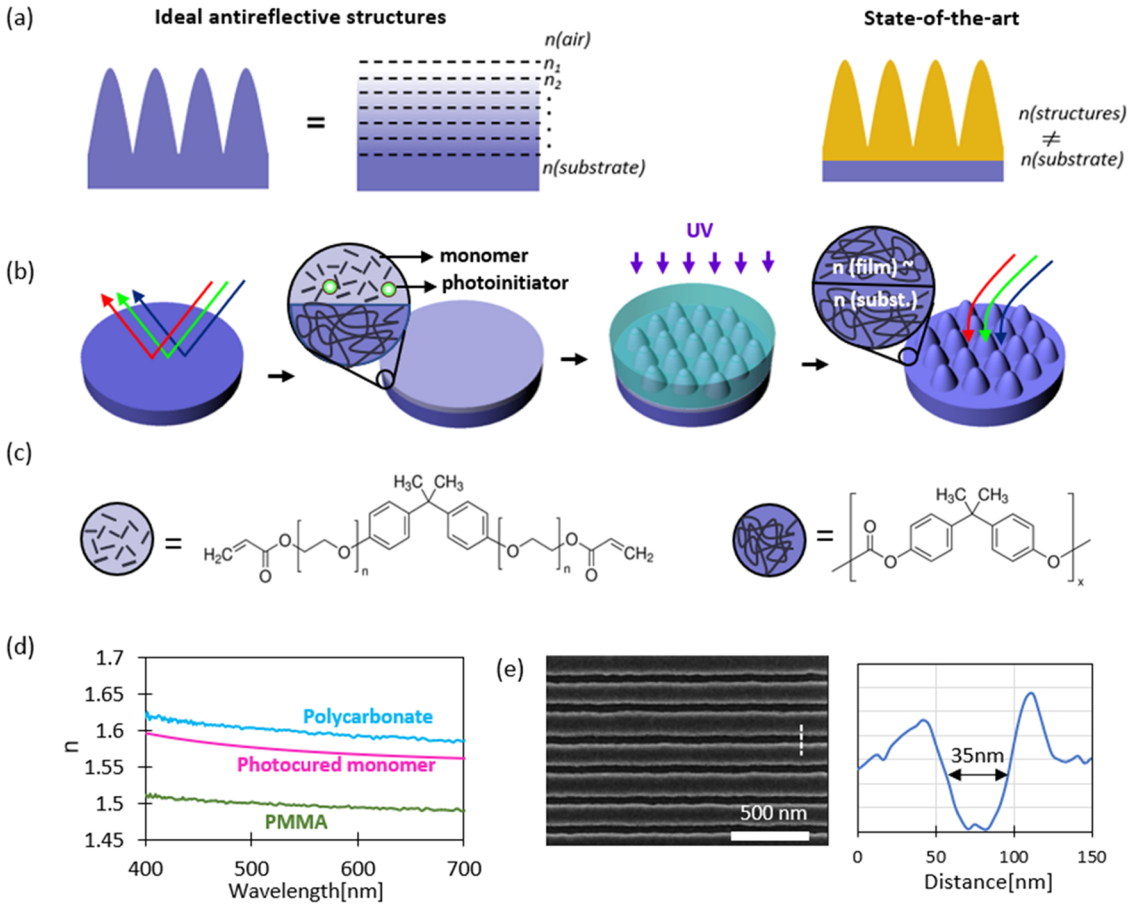

Figure 1. (a) Ideal moth-eye structures vs state-of-the-art moth-eye structures imprinted on the polymer. (b) Schematic process flow of the fabrication of moth-eye structures from an index-matched monomer. The inset shows the chemical structures of the bisphenol A ethoxylate diacrylate monomer and the polycarbonate (c) structure of the polymer and monomer used for UV imprint. (d) Dispersion curves of photocured bisphenol A ethoxylate diacrylate, compared to those of polycarbonate and PMMA. (e) Example of a high-resolution nanoimprint in a photocured bisphenol A ethoxylate diacrylate film of nanoscale lines.

layers. It is clear that optimal antireflective structures must be imprinted within a material whose chemical composition and structure are similar to those of the substrate, as well as the optical properties, including refractive indexes. However, such index-matching between the polymer and imprinted structures has not been demonstrated so far.

Here, we demonstrate highly effective imprinted moth-eye antireflective structures on polymers, achieved by precise index-matching between the polymer and the imprinted structures. To that end, we developed a new strategy to engineer an index-matching imprint material, which is based on a monomer analogous to that of the repeating unit of the polymer, to which we added a UV curing agent. In this way, we achieved an index-matching of down to 0.01 between the polymer and the UV-imprinted monomer. We then used this new imprint material to produce moth-eye structures on the bulk polymer, thereby reducing its reflection from ∼5 to ∼0.1% and increasing its transmission from 88 to 95%. As a negative control, we also produced the same moth-eye structures on another polymer whose refractive index was quite different from that of a photocurable monomer. As expected, in this case, the moth-eye antireflective structures were not as effective as in the case of the index-matching polymer. The effect of index-matching was also confirmed by optical simulations for both polymers, confirming that precise tuning of the refractive index is crucial for the material choice for antireflective structures. We also demonstrated that these moth-eye structures could be applied not only to flat surfaces but also to curved optical surfaces such as lenses. Overall, our findings open a new perspective for the scalable and highly effective antireflective solution for polymer optics.

2. RESULTS AND DISCUSSION

In this work, we chose to use polycarbonate (PC)—a polymer broadly used in optics due to its high transparency in the visible spectrum and good mechanical stability[26]—as the studied optical substrate. We also chose bisphenol A ethoxylate diacrylate as a raw material for the moth-eye layer on polycarbonate based on two hypotheses. The first hypothesis states that because the chemical structure of bisphenol A ethoxylate diacrylate is similar to that of the repeating unit of the polycarbonate, the product of its polymerization will have the same refractive index as the polycarbonate. The second hypothesis postulates that because bisphenol A ethoxylate diacrylate ($M_n \sim 512$) is a viscous liquid with a viscosity in the range of 800−1200 cps at 25 °C, it can be easily UV-nanoimprinted at room temperature to produce a high-resolution pattern. To verify the first hypothesis, we prepared a thin film of photopolymerized bisphenol A ethoxylate diacrylate on a piece of silicon wafer. For this purpose, we added a small amount of commercial photoinitiator to an ethanol-based solution bisphenol A ethoxylate diacrylate,[27]

https://doi.org/10.1021/acsapm.3c00573
ACS Appl. Polym. Mater. 2023, 5, 5103−5109

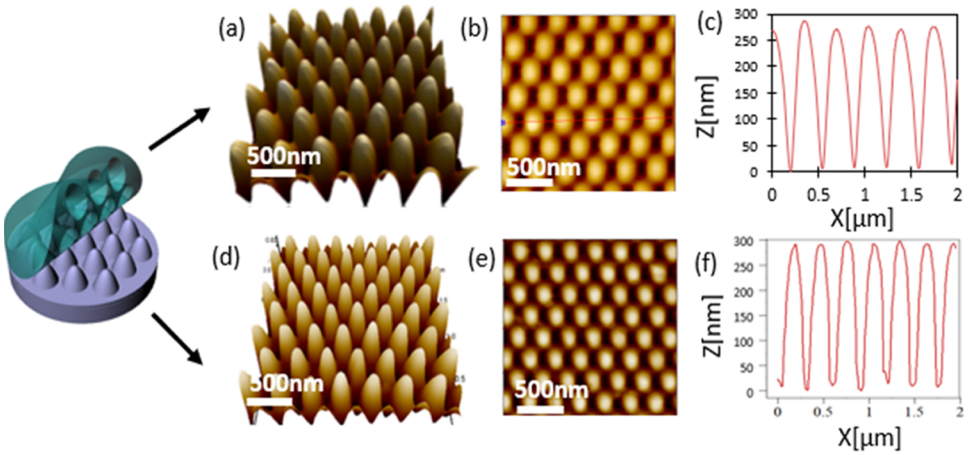

Figure 2. Three-dimensional (3D), top view, and X-section AFM, respectively, of (a–c) the nanoimprint mold. (b–f) Moth-eye structures UV-imprinted in photocured bisphenol A ethoxylate diacrylate.

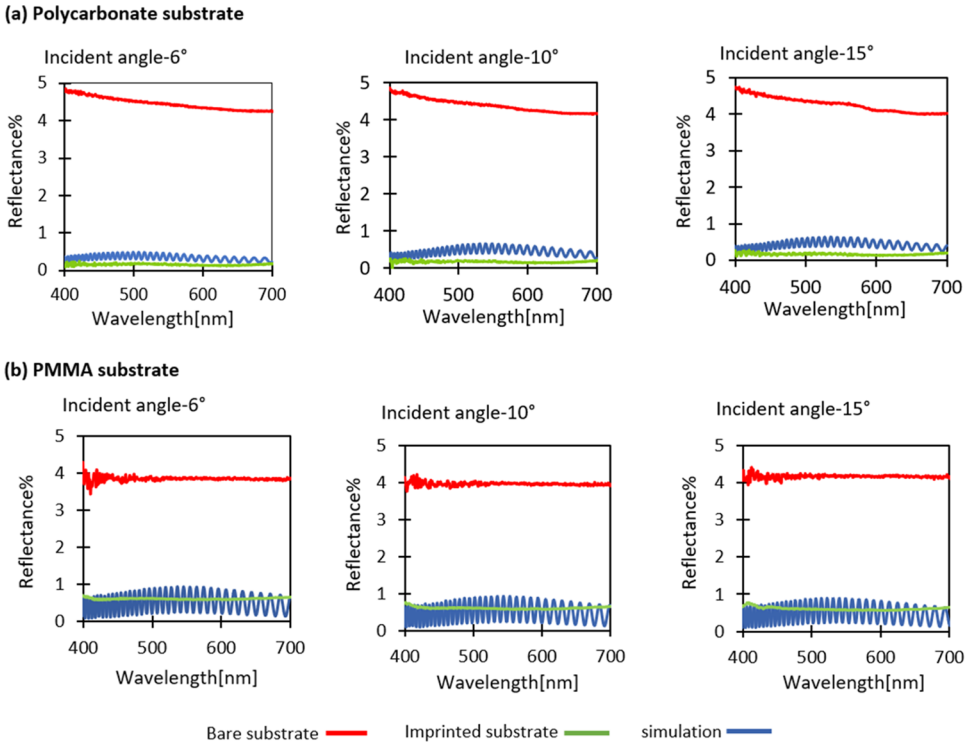

Figure 3. Reflection spectra of (a) polycarbonate and (b) PMMA for different angles of incidence. Red, bare substrates; green, moth-eye structures, and blue, simulation of moth-eye structures.

spin-coated the obtained mixture on a silicon wafer, heated it on a hot plate to remove the residuals of the solvent, and exposed it to UV light to achieve complete curing (see details in Materials and Methods). The resulting film was ~0.5 μm thick, as measured by profilometry. We then used ellipsometry to obtain the dispersion of the refractive index of the obtained film, as well as of the bare polycarbonate and PMMA (Figure 1d). As expected, the spectra of polybisphenol A ethoxylate diacrylate and polycarbonate are almost identical, with a negligible difference of a few percents in the visible range. The index dispersion of polybisphenol A ethoxylate diacrylate was quantified by a Cauchy model and was found to be approx. given by $n = 1.548 + (6280/\lambda^2) + ((21.9 \times 10^7)/(\lambda^4))$, (mean square error of 0.76), as compared to that of polycarbonate given by $n = 1.558 + 9385.26/\lambda^2$.[28]

To verify the second hypothesis, we first produced a hybrid PDMS mold[29] by replication from an electron-beam patterned master containing various patterns with minimal feature size down to 35 nm. Using this mold, we imprinted the spin-coated and baked film of bisphenol A ethoxylate diacrylate containing a photoinitiator in a commercial UV imprint tool. We found that the nanometric features can be replicated in a nano-imprinted bisphenol A ethoxylate diacrylate film with a very high pattern transfer fidelity. This minimal feature size is comparable to that achieved with standard commercial UV imprint resists,[30] and it confirms that photocurable bisphenol A ethoxylate diacrylate can be used to produce an imprinted pattern with any arbitrary geometry, as shown in the Supporting Information (Figure S1).

https://doi.org/10.1021/acsapm.3c00573
ACS Appl. Polym. Mater. 2023, 5, 5103–5109

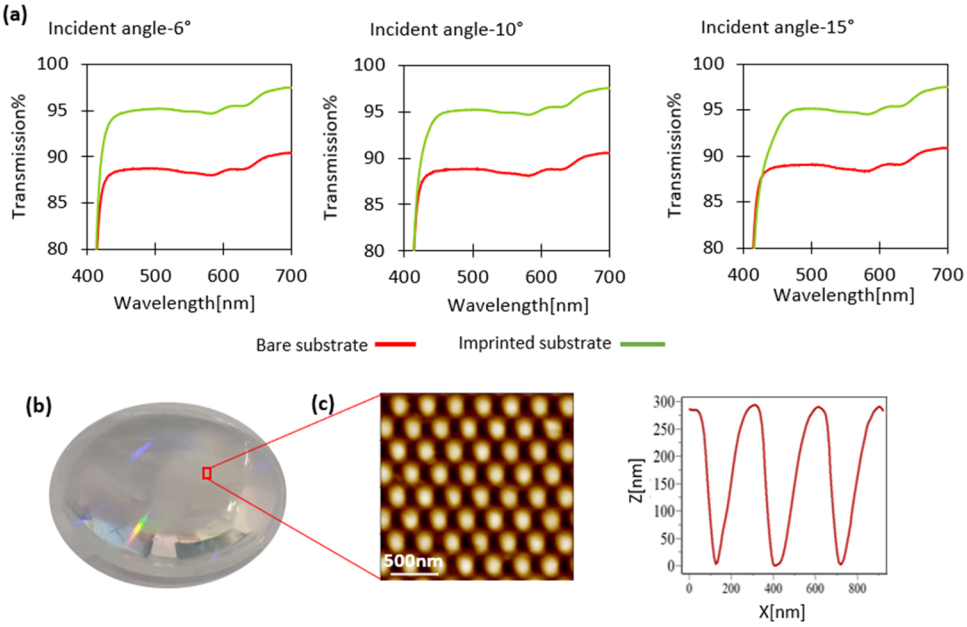

Figure 4. (a) Moth-eye antireflective coating on the surface of the polycarbonate substrate. Transmission spectra of bare (red) and imprinted (green) polymer substrates. (b) Photographic image of a full-cover lens with imprinted antireflective structures. (c) Two-dimensional (2D) and 3D AFM of nanoimprinted polycarbonate.

We then used the same imprinting process to produce moth-eye antireflective structures on polycarbonate. To that end, we used a commercial master mold with periodic conical structures (NIL Technologies), from which we replicated a soft-hard PDMS-based mold as described previously. We then spin-coated an ethanol-based solution of photocurable bisphenol A ethoxylate diacrylate on a sample of polycarbonate (optical grade, 2 cm × 2 cm, size 2 mm thickness), baked it, and imprinted it using the same process condition as described in the previous section. The pattern fidelity of the imprinting process was verified by comparing atomic force microscope (AFM) images of the mold (Figure 2a) and the imprinted pattern (Figure 2d). It can be seen that the features whose vertical dimensions and periodicity on the mold were ∼300 and 300 nm, respectively, were completely and precisely transferred to the imprinted material.

The ability of the imprinted moth-eye structures to reduce the reflection of polycarbonate was characterized by spectrophotometry at different angles of incidence (Figure 3a). The three graphs show the measured specular reflection spectra of bare polycarbonate and polycarbonate imprinted with moth-eye structures for 6, 10, and 15°. Remarkably, the backside of the imprinted polycarbonate was ground with sandpaper prior to the measurement to eliminate backside reflection. Structuring the surface of the polycarbonate with the moth-eye morphology produced the reflection ∼0.1% for an incident angle of 6°. This reflection is extremely low compared to $t \sim 5\%$ reflection of bare polycarbonate, which is was obained by measurement an by calculation based on its dispersion (Figure S2). As expected, the reflection increases for the higher angles of incidence, yet it still stays mostly below 0.2% even for the 15° incident angle. This reduction in the reflection of the polymer by moth-eye structures is unprecedented, and it is strikingly greater than all of the previously reported moth-eye structures on polymers.[17] Indeed, a state-of-the-art moth-eye antireflective structure imprinted on a polymer could reduce the reflection of polycarbonates only by half.[16] The reduction in the reflection we achieved is also superior to that achieved by moth-eye structures fabricated by thermal imprinting on a polymer.[31] This experimentally obtained antireflective effect greatly matches that predicted by simulations, which we have done using software developed in-house that is based on the effective medium theory.[32] This theory does not take scattering into account, yet it can still sufficiently predict the antireflective behavior of the structures with the used periodicity.[33] These simulations considered the precise geometry of the obtained moth-eye structures, as well as the residual layer of the imprinted material. Notably, the oscillations in the simulated spectra are due to resonance in the residual layer of the imprinted material, whose thickness is in the range of a few microns. These oscillations, however, do not appear in the experimental spectra, most probably due to the nonuniformity in the thickness of the residual layer. In addition, to emphasize that the observed antireflective effect was due to the imprinted structure, we measured the reflection of the plain cross-linked film of the monomer on a polycarbonate and found that it is nearly identical to that of a bare polycarbonate (Figure S3)

To verify that the matching in the indices of the substrate and the imprinting material is critical for obtaining an antireflective effect, we repeated these experiments with a PMMA substrate, whose index, as shown before, is different from that of the photocured photocurable bisphenol A ethoxylate diacrylate by ∼0.1. The reflection spectra are shown in Figure 3b. It is clearly seen that in contrast to polycarbonate, here, the reflection was reduced to the range of 0.6−0.7%, both experimentally and by simulations. Since all of the parameters of the antireflective structures were the same as previously, it is obvious that the mismatch in the refractive index is the only reason for such a relatively lower antireflective effect. Still, the obtained antireflective effect could be sufficient for many practical applications. Of course, this reflectivity can be further reduced by using an imprint material whose index sufficiently matches that of PMMA.

https://doi.org/10.1021/acsapm.3c00573
ACS Appl. Polym. Mater. 2023, 5, 5103−5109

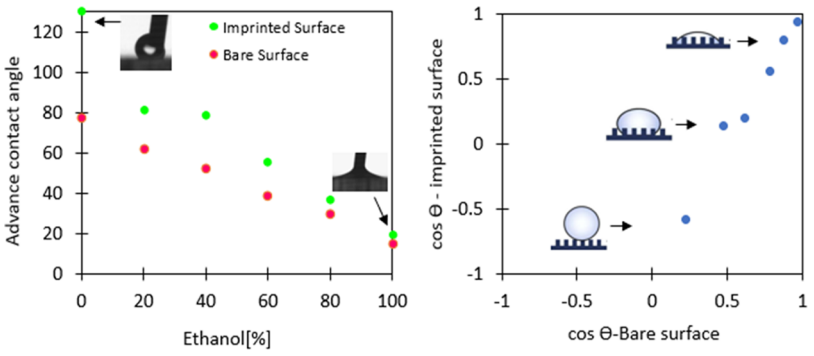

Figure 5. Wetting properties of the imprinted polycarbonate surface. (a) Advancing contact angles of the water−ethanol mixture for imprinted and bare surfaces. (b) Wetting diagram indicating the transition between different wetting states of the imprinted surface.

To demonstrate the attractiveness of the described imprinting approach for polymer-based refractive optics, we assessed the ability of the fabricated moth-eye structures to improve the transmission of polymer optical substrates. To that end, we sequentially imprinted bisphenol A ethoxylate diacrylate moth-eye structures on both sides of the polycarbonate and characterized the polycarbonate transmission for different angles of incidence (Figure 4a). The fabricated structures increased the transmission by about ∼7% up to ∼98% for the highest part of the visible spectrum. Interestingly, this value of transmission is lower than what could be expected based on the ultralow reflection shown in Figure 3. Therefore, there are some losses of the optical signal beyond those caused by reflection. We attribute these losses to scattering, which was likely caused by the periodicity of the imprinted structures that were at the same scale as the wavelength. As mentioned above, this scattering was not considered in the effective medium theory that was at the base of the optical simulations in this work. Experimentally, this scattering can be minimized by reducing the periodicity of the imprinted structures to a size a few times smaller than the wavelength. The minimal feature size of 35 nm demonstrated here confirms that imprinting such structures is easily achievable by the fabrication approach described here.

To date, we have demonstrated the fabrication of the moth-eye structures on flat substrates. However, the great advantage of soft imprinting is that it can be applied to curved substrates. In the context of polymer optics, this unique feature of soft imprint makes the fabrication described here attractive for producing antireflective structures on curved optical components, such as lenses. Here, we produced moth-eye structures on the surface of a convex lens using exactly the same methodology as described previously for flat surfaces. The diameter of the lens was 3.4 cm, and the radius of curvature was 3.2 cm. Figure 4b shows a photograph of the imprinted lens, and Figure 4c shows the 3D and cross-section AFM of the imprinted structure taken at the center of the lens. The uniform imprint on the lens surface was possible due to the used commercial tool (Nanonex B200), which applies isotropic pneumatic pressure on the soft mold through the elastic membrane. It is seen from the AFM that the dimensions of the imprinted features correspond to those of the features on the mold, as observed previously for the imprint on a flat surface. On the other hand, the periodicity of the imprinted structures should be, in principle, affected by the curvature of the substrate due to the stretching of the soft mold induced by the full contact with the substrate. To verify that the geometry of the imprinted structures is uniform through the lens surface, we scanned the lens surface in a position located 1 cm away from its center and found that the structure geometry is identical to that in the center of the lens (Figure S4). Therefore, if there is any possible effect of the mold stretching on the imprinted structure, it is negligible.

Finally, besides the antireflective effect, the imprinted nanostructures are also supposed to be water-repellent.[34] This water-repellence is also inspired by nature and is often called the "lotus leaf effect".[35] Such an effect is beneficial for optical surfaces since it prevents continuous contamination that originates from ongoing condensation and evaporation of water. The combination of antireflective and self-cleaning properties of nanostructured surfaces has been studied before on various optical materials.[36] Here, we demonstrate that moth-eye structures UV-imprinted on a polymer possess similar hydrophobic properties, which, in turn, can contribute to the long-term stability of optical devices onto which these moth-eye structures are implemented. To characterize the hydrophobicity of the imprinted polycarbonate, we assessed the advancing contact angle (ϑ) of water−ethanol mixtures at different ratios and compared them to those of bare polycarbonate (Figure 5a). As expected, for most of the liquid compositions, there was not a high difference between the patterned and nonpatterned surfaces. Yet, the difference for pure water was striking—from 77° on a flat polycarbonate to 130° on a patterned polycarbonate. To analyze this superhydrophobic effect, we plotted $\cos(\vartheta)$ of the moth-eye surface vs $\cos(\vartheta)$ of the flat polycarbonate (Figure 5b).[36] The obtained plot fits the well-established model of wetting on a surface covered with fractal structures.[37] Here, the points in the upper right corner can be attributed to the Wenzel state, in which the surface morphology is entirely wetted by the liquid. On the other hand, the point on the bottom part of the graph can be attributed to the Cassie−Baxter state, in which the liquid incompletely wets the surface due to the air traps between the structures.[38]

In summary, we demonstrated here an innovative and facile approach for highly effective and robust moth-eye antireflective structures on polymer surfaces. At the crux of our invention is the matching between the indices of the optical surface and the material for the moth-eye relief structures. Due to this innovation, we achieved an unprecedented reduction in surface reflection, which reached its theoretical limit. By varying different optical substrates using the same imprint material, we demonstrated the critical importance of the choice of a moth-eye material with the same index. Our approach was

https://doi.org/10.1021/acsapm.3c00573
ACS Appl. Polym. Mater. 2023, 5, 5103−5109

demonstrated on a specific pair of materials—polycarbonate for the substrate and photopolymerized bisphenol A ethoxylate diacrylate for the imprint. However, the great variety of liquid optical materials and curing agents available in today's market enables one to fit an appropriate photo-imprint-able material for any optical substrate and for any spectral range. The demonstrated ability to imprint a curved lens paves the way to the fabrication of antireflective structures on free-form polymer optics, which is an emerging, simple, and cost-effective alternative to complicated systems assembled from distinct optical components. Overall, this work opens a route to numerous applications that require cost-effective yet high-quality polymer-based optical devices and components.

3. EXPERIMENTAL SECTION

3.1. Fabrication of Soft Stamps. Hybrid PDMS soft stamps were replicated from a commercial nickel master patterned with moth-eye conical nanostructures (NIL Technology) by directly casting their precursors onto the patterned master mold. For this purpose, we first mixed 3.4 g of vinyl PDMS prepolymer (VDT-731, Gelest corp), 18 mL of platinum catalyst (platinum divinyltetramethyldisiloxane, SIP6831.2LC Gelest Corp.), and 5 mL of modulator (2,4,6,8-tetramethyl tetravinylcyclotetrasiloxane, Sigma-Aldrich) and degassed the mixture for 1−2 min. We then gently added 1 g of hydrosilane prepolymer (HMS-301, Gelest Corp.) to the mixture, gently stirred it, immediately applied a thin film of the resulting new mixture onto the master by spin-coating, and cured it at 60 °C for 30 min. After cooling the cured film, we poured onto it a mixture of PDMS (Sylgard 184 PDMS, Dow Corning) and its hardening reagent (10:1 v/v), degassed it, and further baked it at 60 °C for 1 h. Finally, we peeled the obtained mold off the master.[29]

3.2. Preparation of the Photocurable Bisphenol A Ethoxylate Diacrylate Film. 1.2 gr of a low-molecular-weight monomer (bisphenol A ethoxylate diacrylate, M_w = 512, sigma) was mixed with 0.02 gr of a photoinitiated powder (2,2-dimethoxy-2-phenylacetophenone 99%, ALDRICH) and 2 mL of ethanol.[27] The mixture was sonicated for 5 min to form a uniform solution. Then, the solution was spin-coated on a 1 in. square polycarbonate substrate, followed by soft baking at 50 °C for 6 min on a hot plate to remove the residual ethanol. Spinning at 7000 rpm for 30 s produced a film thickness of ∼10 μm.

3.3. Direct UV-Nanoimprint. The imprint was done in a Nanonex 200B nanoimprint tool. A coated polymer surface with a photocurable film was first brought in contact with a soft stamp. The two were placed between two silicone elastomeric membranes and positioned inside the pressure chamber. The chamber was vacuumed to prevent the formation of air bubbles between the imprinted surface and the stamp. Then, the substrate was heated to 35 °C, and a pressure of 400 psi was applied, along with UV light, for 10 min. Finally, the chamber was left to cool gradually to room temperature. The imprinted patterns were characterized by AFM (FlexAFM, Nanosurf).

3.4. Optical Measurements. The reflection and transmission spectra of the imprinted and bare polymer samples were measured in the visible range using a spectrophotometer (Cary 5000, Agilent) at three different angles: 6, 10, and 15°. For reflection measurements, the backside of the samples was ground with sandpaper to cancel the reflection of the backside. For the transmission measurements, both sides of the samples were patterned with moth-eye structures. The refractive index of the photocured bisphenol A ethoxylate diacrylate was measured by an ellipsometer tool (spectra ray) in the wavelength range of 400−850 nm and 70° angle of incidence.

3.5. Optical Simulations. The simulations were done using a MATLAB code based on the effective medium theory. For the calculation of the reflectance, the textured medium is replaced by an effective medium consisting of 40 stacked films of equal thickness. For each film, the effective refractive index is calculated using the Maxwell−Garnett formula.[32] The reflectance of this structure is then calculated using the transfer matrix method.[22]

ASSOCIATED CONTENT

Supporting Information

The Supporting Information is available free of charge at https://pubs.acs.org/doi/10.1021/acsapm.3c00573.

Additional data, including examples of nanoimprinted structures, reflection spectra of bare polymer substrates, and micrograph of antireflective structures imprinted on a polymer lens (PDF)

AUTHOR INFORMATION

Corresponding Author

Mark Schvartzman − *Department of Materials Engineering and Ilse Katz Institute for Nanoscale Science & Technology, Ben-Gurion University of the Negev, Beer-Sheva 84105, Israel*; orcid.org/0000-0002-5912-525X; Email: marksc@bgu.ac.il

Authors

Sivan Tzadka − *Department of Materials Engineering and Ilse Katz Institute for Nanoscale Science & Technology, Ben-Gurion University of the Negev, Beer-Sheva 84105, Israel*

Imon Kalyan − *Department of Electrical Engineering, Ben-Gurion University of the Negev, Beer-Sheva 84105, Israel*

Esti Toledo − *Department of Materials Engineering and Ilse Katz Institute for Nanoscale Science & Technology, Ben-Gurion University of the Negev, Beer-Sheva 84105, Israel*; orcid.org/0000-0003-3103-816X

Yonatan Sivan − *Department of Electrical Engineering, Ben-Gurion University of the Negev, Beer-Sheva 84105, Israel*; orcid.org/0000-0003-4361-4179

Complete contact information is available at: https://pubs.acs.org/10.1021/acsapm.3c00573

Funding

This work was supported by the Israel Innovation Authority, KAMIN program.

Notes

The authors declare no competing financial interest.

REFERENCES

(1) Ma, H.; Jen, A. K.-Y.; Dalton, L. R. Polymer-Based Optical Waveguides: Materials, Processing, and Devices. *Adv. Mater.* **2002**, *14*, 1339−1365.

(2) Loste, J.; Lopez-Cuesta, J. M.; Billon, L.; Garay, H.; Save, M. Transparent Polymer Nanocomposites: An Overview on Their Synthesis and Advanced Properties. *Prog. Polym. Sci.* **2019**, *89*, 133−158.

(3) Althues, H.; Henle, J.; Kaskel, S. Functional Inorganic Nanofillers for Transparent Polymers. *Chem. Soc. Rev.* **2007**, *36*, 1454−1465.

(4) Raut, H. K.; Ganesh, V. A.; Nair, A. S.; Ramakrishna, S. Anti-Reflective Coatings: A Critical, in-Depth Review. *Energy Environ. Sci.* **2011**, 3779−3804.

(5) Han, X.-Y.; Wu, Z.-L.; Yang, S.-C.; Shen, F.-F.; Liang, Y.-X.; Wang, L.-H.; Wang, J.-Y.; Ren, J.; Jia, L.-Y.; Zhang, H.; Bo, S.-H.; Morthier, G.; Zhao, M.-S. Recent Progress of Imprinted Polymer Photonic Waveguide Devices and Applications. *Polymers* **2018**, *10*, No. 603.

(6) Oh, S. S.; Choi, C. G.; Kim, Y. S. Fabrication of Micro-Lens Arrays with Moth-Eye Anti-reflective Nanostructures Using Thermal Imprinting Process. *Microelectron. Eng.* **2010**, *87*, 2328−2331.

(7) Pina-Hernandez, C.; Koshelev, A.; Dhuey, S.; Sassolini, S.; Sainato, M.; Cabrini, S.; Munechika, K. Nanoimprinted High-Refractive Index Active Photonic Nanostructures Based on Quantum Dots for Visible Light OPEN. *Sci. Rep.* **2017**, *7*, No. 17645.
(8) Bender, M.; Otto, M.; Hadam, B.; Vratzov, B.; Spangenberg, B.; Kurz, H. Fabrication of Nanostructures Using a UV-Based Imprint Technique. *Microelectron. Eng.* **2000**, *53*, 233−236.
(9) Cui, B.; Veres, T. Pattern Replication of 100 Nm to Millimeter-Scale Features by Thermal Nanoimprint Lithography. *Microelectron. Eng.* **2006**, *83*, 902−905.
(10) Shan, X. C.; Ikehara, T.; Murakoshi, Y.; Maeda, R. Applications of Micro Hot Embossing for Optical Switch Formation. *Sens. Actuators, A* **2005**, *119*, 433−440.
(11) Jiao, F.; Huang, Q.; Ren, W.; Zhou, W.; Qi, F.; Zheng, Y.; Xie, J. Enhanced Performance for Solar Cells with Moth-Eye Structure Fabricated by UV Nanoimprint Lithography. *Microelectron. Eng.* **2013**, *103*, 126−130.
(12) David, C.; Häberling, P.; Schnieper, M.; Söchtig, J.; Zschokke, C. Nano-Structured Anti-Reflective Surfaces Replicated by Hot Embossing. *Microelectron. Eng.* **2002**, *61*−*62*, 435−440.
(13) Jacobo-Martín, A.; Rueda, M.; Hernández, J. J.; Navarro-Baena, I.; Monclús, M. A.; Molina-Aldareguia, J. M.; Rodríguez, I. Bioinspired Antireflective Flexible Films with Optimized Mechanical Resistance Fabricated by Roll to Roll Thermal Nanoimprint. *Sci. Rep.* **2021**, *11*, No. 2419.
(14) Kang, Y. H.; Han, J. H.; Cho, S. Y.; Choi, C.-G. Resist-Free Anti-reflective Nanostructured Film Fabricated by Thermal-NIL. *Nano Convergence* **2014**, *1*, No. 19.
(15) Chen, J.; Cheng, J.; Zhang, D.; Chen, S. C. Precision UV Imprinting System for Parallel Fabrication of Large-Area Micro-Lens Arrays on Non-Planar Surfaces. *Precis. Eng.* **2016**, *44*, 70−74.
(16) Burghoorn, M.; Roosen-Melsen, D.; De Riet, J.; et al. Single Layer Broadband Anti-Reflective Coatings for Plastic Substrates Produced by Full Wafer and Roll-to-Roll Step-and-Flash Nano-Imprint Lithography. *Mater* **2013**, *6*, 3710−3726.
(17) Sun, J.; Wang, X.; Wu, J.; Jiang, C.; Shen, J.; Cooper, M. A.; Zheng, X.; Liu, Y.; Yang, Z.; Wu, D. Biomimetic Moth-Eye Nanofabrication: Enhanced Antireflection with Superior Self-Cleaning Characteristic. *Sci. Rep.* **2018**, *8*, No. 5438.
(18) Jacobo-Martín, A.; Herandez, J.; Pedraz, P.; Solano, E.; Navarro-Baena, I.; Rodriguez, I. Improve thermal stability of anti-reflective moth-eye topography imprinted on PMMA/TiO2 surface nanocomposites. *Nanotechnology* **2021**, *32*, No. 335302.
(19) Hobbs, D. S.; MacLeod, B. D. In *Design, Fabrication, and Measured Performance of Anti-Reflecting Surface Textures in Infrared Transmitting Materials*, Window and Dome Technologies and Materials; SPIE Digital Library, 2005.
(20) Kuo, W.-K.; Hsu, J.-J.; Nien, C.-K.; Yu, H. H. Moth-Eye-Inspired Biophotonic Surfaces with Antireflective and Hydrophobic Characteristics. *ACS Appl. Mater. Interfaces* **2016**, *8*, 32021−32030.
(21) Vandormael, D.; Habraken, S.; Loicq, J.; Lenaerts, C.; Mawet, D. In *Anti-Reflective Sub-Wavelength Patterning of IR Optics*, Electro-Optical and Infrared Systems: Technology and Applications III; SPIE Digital Library, 2006.
(22) Ohta, K.; Ishida, H. Matrix Formalism for Calculation of Electric Field Intensity of Light in Stratified Multilayered Films. *Appl. Opt.* **1990**, *29*, 1952−1959.
(23) Skaar, J. Fresnel Equations and the Refractive Index of Active Media. *Phys. Rev.* **2006**, *73*, No. 026605.
(24) Zhang, J.; Shen, S.; Dong, X. X.; Chen, L. S. Low-Cost Fabrication of Large Area Sub-Wavelength Anti-Reflective Structures on Polymer Film Using a Soft PUA Mold. *Opt. Express* **2014**, *22*, 1842−1851.
(25) Zhou, Y.; Shen, S.; Zhang, J.; Jin, F-P.; Liu, Y-H. Fabrication of Sub-Wavelength Anti-reflective Structures Using a Soft Roll-to-Plate Nanoimprinting Lithographic Method. *Adv. Mater. Res.* **2015**, *1118*, 3−8.
(26) Davis, A.; Golden, J. H. Stability of Polycarbonate. *J. Macromol. Sci., Part C* **2008**, *3*, 49−68.
(27) Anastasio, R.; Peerbooms, W.; Cardinaels, R.; Van Breemen, L. C. A. Characterization of Ultraviolet-Cured Methacrylate Networks: From Photopolymerization to Ultimate Mechanical Properties. *Macromolecules* **2019**, *52*, 9220−9231.
(28) Roth, B.; Wildner, W.; Drummer, D. Analysis of the Processing-Pressure Dependent Refractive Index of Polycarbonate by Transmission Measurements of Glass-Filled Specimen. *Polym. Eng. Sci.* **2020**, *60*, 512−516.
(29) Odom, T. W.; Love, J. C.; Wolfe, D. B.; Paul, K. E.; Whitesides, G. M. Improved Pattern Transfer in Soft Lithography Using Composite Stamps. *Langmuir* **2002**, *18*, 5314−5320.
(30) Guo, L. J. Recent Progress in Nanoimprint Technology and Its Applications. *J. Phys. D: Appl. Phys.* **2004**, *37*, R123−R141.
(31) Rosenberg, M.; Schvartzman, M. Direct Resistless Soft Nanopatterning of Freeform Surfaces. *ACS Appl. Mater. Interfaces* **2019**, *11*, 43494−43499.
(32) Choy, T.*Effective Medium Theory: Principles and Applications*; Oxford University Press, 2015; Vol. *165*.
(33) Fung, T. H.; Veeken, T.; Payne, D.; Veettil, B.; Polman, A.; Abbott, M. Application and Validity of the Effective Medium Approximation to the Optical Properties of Nano-Textured Silicon Coated with a Dielectric Layer. *Opt. Express* **2019**, *27*, 38645−38660.
(34) Tzadka, S.; Ostrovsky, N.; Toledo, E.; Le Saux, G.; Kassis, E.; Joseph, S.; Schvartzman, M. Surface Plasticizing of Chalcogenide Glasses: A Route for Direct Nanoimprint with Multifunctional Anti-reflective and Highly Hydrophobic Structures. *Opt. Express* **2020**, *28*, 28352−28365.
(35) Quéré, D. Wetting and Roughness. *Annu. Rev. Mater. Res.* **2008**, *38*, 71−99.
(36) Park, K. C.; Choi, H. J.; Chang, C. H.; Cohen, R. E.; McKinley, G. H.; Barbastathis, G. Nanotextured Silica Surfaces with Robust Superhydrophobicity and Omnidirectional Broadband Supertransmissivity. *ACS Nano* **2012**, *6*, 3789−3799.
(37) Shibuichi, S.; Onda, T.; Satoh, N.; Tsujii, K. Super Water-Repellent Surfaces Resulting from Fractal Structure. *J. Phys. Chem. A* **1996**, *100*, 19512−19517.
(38) Onda, T.; Shibuichi, S.; Satoh, N.; Tsujii, K. Super-Water-Repellent Fractal Surfaces. *Langmuir* **1996**, *12*, 2125−2127.

https://doi.org/10.1021/acsapm.3c00573
ACS Appl. Polym. Mater. 2023, 5, 5103−5109